Aberration evaluation and tolerancing of 193nm lithographic objective lenses

Bruce W. Smith[a], James Webb[b], John S. Petersen[c], Jeff Meute[c]
[a]Rochester Institute of Technology, 82 Lomb Memorial Dr., Rochester, N.Y. 14623-5604
[b]Tropel Corporation, Fairport, N.Y 14450, [c]SEMATECH, Austin, TX 78741
[a]bwsemc@rit.edu

ABSTRACT

Described here is an approach to aberration tolerancing utilizing aerial image parameterization based on photoresist capability. A minimum aerial image metric is determined from either a characterized resist process or desirable resist attributes and includes definition of resist exposure, diffusion, and development properties. Minimum aerial image requirements can then be correlated to resist performance to allow for the evaluation of various feature sizes and types. This allows, for example, the prediction of lens performance through focus, across the field, and in the presence of small levels of internal flare. Results can then be compared with more conventional optical metrics such as Strehl ratio, partial coherence contrast, or image threshold CD.

Results are presented for three commercial small field catadioptric 193nm lithographic lenses. Aberration levels for each lens at several field positions and at several wavelengths has been described using 37. Zernike polynomial coefficients. Minimum aerial image requirements have been correlated to resist performance to allow the evaluation of various feature types, a unique situation when no mature 193nm resist process existed. Additionally, the impact of modified illumination on aberrations is presented.

1. INTRODUCTION

At some point during the design and testing of an optical lithographic system, a definition of image recording processes is required As lithographic lenses are built to perform at increasingly higher levels of resolution, requirements for numerical aperture, wavelength, focal depth, and aberration level need to be well understood. An understanding of the relationships between the optical and photoresist requirements of microlithographic image formation is becoming increasingly important. During steps of optical parameter optimization and aberration tolerancing, a connection is needed between aerial images produced by the optical system and final photoresist image. First order metrics are not adequate for more than basic insight. A description of optical lens aberration through wavefront deformation can be incorporated into modeling processes using data acquired through phase-measurement interferometry (PMI) techniques but sufficient knowledge of a the resist process is needed for complete analysis. It is often difficult to obtain the required information to make the connection between image and photoresist performance, since doing so involves a fully developed resist process and a tremendous amount of experimental iteration.

1.1 ABERRATION TOLERANCING

For OPDs less than a few wavelengths of light, aberration levels can be considered small. Since any amount of aberration results in image degradation, tolerance levels must be established for lens system, dependent on application. This results in the need to consider not only specific object requirements and illumination but also resist requirements. For microlithographic application, resist and process capability will ultimately influence allowable lens aberration level.

Conventionally, a diffraction limited lens is one which produces no more than one quarter wavelength ($\lambda/4$) wavefront OPD. For many non-lithographic lens systems, the reduced performance resulting from this level of aberration is allowable. The current requirements of lithographic imaging place demands that are near an order of magnitude tighter than this. To measure image quality as a result of lens aberration, the distribution of energy in an intensity point spread function (PSF) can be evaluated. The ratio of energy at the center of an aberrated point image to the energy at the center of a unaberrated point image is known as the Strehl ratio. For an aberration free lens, of course, the Strehl ratio is 1.0. For a lens with $\lambda/4$ OPD, the Strehl ratio is 0.80, nearly independent of the specific aberration present. This is conventionally known as the Rayleigh $\lambda/4$ rule [1]. Strehl ratio can be used to understand a good deal about an imaging process. The PSF is fundamental to imaging theory and can be used to calculate the diffraction image of both coherent and incoherent objects.

By convolving a scaled object with the lens system PSF, the resulting incoherent image can be determined. In effect, this becomes the summation of the irradiance distribution of the image elements. Similarly, a coherent image can be determined by adding the complex amplitude distributions of the image elements. The optical transfer function (OTF) is often used to evaluate the relationship between an image and the object that produced it [2]. In general, a transfer function is a description of an entire imaging process as a function of spatial frequency. It is a scaled Fourier transform of the PSF of the system. The concept of critical modulation is a useful approximation for relating minimum image modulation required for a photoresist material. The minimum required modulation for a resist with contrast γ can be determined as $(e^{1/\gamma}-1)/(e^{1/\gamma}+1)$.

For practical application, a lens requires a set of OTFs, one for each unique isoplanatic region or zone position. The number of OTFs required for any lens will be a function of required performance and financial or technical capabilities. Although a large number of OTFs will better characterize a lens, more than a few may be impractical. Since an OTF will degrade with defocus, a position of best focus would normally be chosen for lens characterization. To extend evaluation of aberrated images for partially coherent systems, the use of the PSF or an OTF becomes difficult. The general rule of thumb that the effects on image quality is similar for identical levels of primary wavefront aberration also becomes invalid for microlithographic application since small changes in image shape, size, or position can significantly impact performance. Methods of aerial image simulation can be utilized for lens performance evaluation. By incorporating lens aberration parameters into a scalar or vector diffraction model, most appropriately though use of Zernike polynomial coefficients, aerial image metrics such as image modulation or normalized image log-slope (NILS) can be used.

1.2. AERIAL IMAGE METRICS

OTF or comparable metrics are limited to periodic features or gratings of equal lines and spaces. Other metrics may be used for the evaluation of image quality by measuring some aspect of an aerial image with less restriction on feature type. These may include measurements of image energy, image shape fidelity, critical image width, and image slope. Since feature width is a critical parameter for lithography, aerial image width is a useful metric for insight into performance of resist images. A 30% intensity threshold is commonly chosen for image width measurement [3]. Few of these metrics, though, give an adequate representation of the impact of aerial image quality on resist process latitude.

Through measurement of the aerial image log-slope normalized to feature size or NILS, an indication of resist process performance can be obtained . Since an exposure profile leads to a resist profile upon development, measurement of the NILS can be directly related to a resist image. Changes in this log aerial image gradient will therefore directly influence resist profile and process latitude.

To determine the minimum usable NILS values for use with a photoresist process, resist requirements need to be considered. As the minimum image modulation requirement has been related above to resist contrast properties, there must also a relationship between resist performance and minimum NILS requirements. Since bulk resist properties such as contrast may not adequately relate to process specific responses such as feature size control, exposure latitude, or DOF, more suitable evaluation methods may be desirable.

2. DETERMINING MINIMUM IMAGING REQUIREMENTS

A transfer model approach can be used to describe a lithographic process from aerial image creation to final resist profile, similar to those introduced for photographic systems by Jones [4]. The usefulness of this transfer approach to lithographic modeling is seen as process requirements are incorporated. A photoresist process is chosen with contrast (γ) , capable of printing features with maximum aspect ratio *AR*. A specification is placed on the minimum acceptable resist sidewall angle (*SA*), below which resist features are no longer considered to be resolved. The minimum image log slope can be determined as:

$$CD \times ILS_{\min} = \frac{\tan(SA)}{\gamma AR} = NILS_{\min}$$

By considering a requirement for exposure latitude (EL), NILS is no longer measured at the mask edge but at positions near the mask edge (ME):

$$\text{Effective edge} = ME + \left[\frac{\pm EL}{NILS_{ME}} \right]$$

While a measure of resist gamma is sufficient for description of the dense feature capabilities of a resist material, it is not well suited for the evaluation of non-periodic geometry. Also, resist gamma becomes an inadequate description for current resist materials, especially those which undergo chemical amplification and possess non-linear exposure and dissolution properties. Allowance for tolerable deviations in feature size is also difficult to incorporate. The imaging performance of isolated line, space, contact, and island geometry is important and to evaluate non-periodic geometry, feature specific metrics need to be addressed. A set of NILS values can then exist, each value unique for a given feature type. Generally, when a photoresist process is characterized, a series of resist images are produced at various exposure levels and through a range of focus values. Tolerable limits are placed on CD and exposure latitude to allow for determination of a usable depth of focus. Through extraction of photoresist process parameters, modeling of the exposure and development of a resist process is possible. An entire lithographic process can then be simulated using such a resist model tied together with a suitable scalar or vector diffraction imaging model. This allows for determination of feature specific aerial image requirements.

2.1 EXPANDING RESIST MODELING FOR PARAMETER TOLERANCING

To establish a set of minimum NILS values for various geometry types, lithographic modeling is utilized[5]. This situation has been unique as imaging parameters (including aberration at various field positions) were well known yet a mature 193nm resist process did not exist. Desired attributes of a 193nm single layer resist were extracted from a parameterized 248 nm single layer resist process[6]. These resist and process parameters are shown in Table 1.

1050.00	;Development Rmax (nm/s)	1	;Exposed Diffusivity rel. to Unexposed
0.400	;Development Rmin (nm/s)	0.000	;Room Temperature Acid Diff. Length (nm)
0.48	;Development Mth		
11.000	;Development n	1.0000	;Amplification Reaction Order
.1	;Surface Development Rate	0.0001	;Relative Surface Contam. Conc.
150.000	;Inhibition Depth (nm)	80.000	;Contamination Diff. Length (nm)
1.769	;Refractive index at 193nm	0.15	;Relative Quencher Concentration
0.52	;absorption (1/um) at 193 nm	39.623	;PEB Amplification Ea (kcal/mole)
0.051	;Dill C (cm2/mJ) at 193nm	47.818	;PEB Amplification ln(Ar) (1/s)
35.000	;Thermal Decomp. Ea (kcal/mole)	25.00	;PEB Diffusion Rate Constant, σ Ea (kcal/mole)
30.000	;Thermal Decomp. ln(Ar) (1/s)	45.00	;PEB Diffusion Rate Constant ln(Ar) (1/s)
39.623	;PEB Diffusivity Ea (kcal/mole)		
54.315	;PEB Diffusivity ln(Ar) (nm2/s)	39.623	;PEB Bulk Acid Loss Ea (kcal/mole)
1	;Diffusivity Variation (1=linear)	45.6	;PEB Bulk Acid Loss ln(Ar) (1/s)

Table 1. Resist / process parameters used for 193nm resist modeling, based on a 248 nm CAR.

Figures 1 and 2 show how focus-exposure matrices along with aerial image log-slope vs. focus curves can allow for estimation of aerial image requirements. A process CD specification of +/- 10% and an exposure latitude requirement of 10% have been imposed on both dense (1:1) and isolated 0.16 μm line processes (193 nm, 0.6NA, 0.7σ). The resulting usable depth of focus can then be traced through aerial image vs. defocus relationships to determine minimum NILS requirement. The minimum NILS value for dense lines is 2.4 and the minimum NILS value for isolated lines is 2.1. Process improvements or relaxation of process requirements can lead to acceptable NILS below these values.

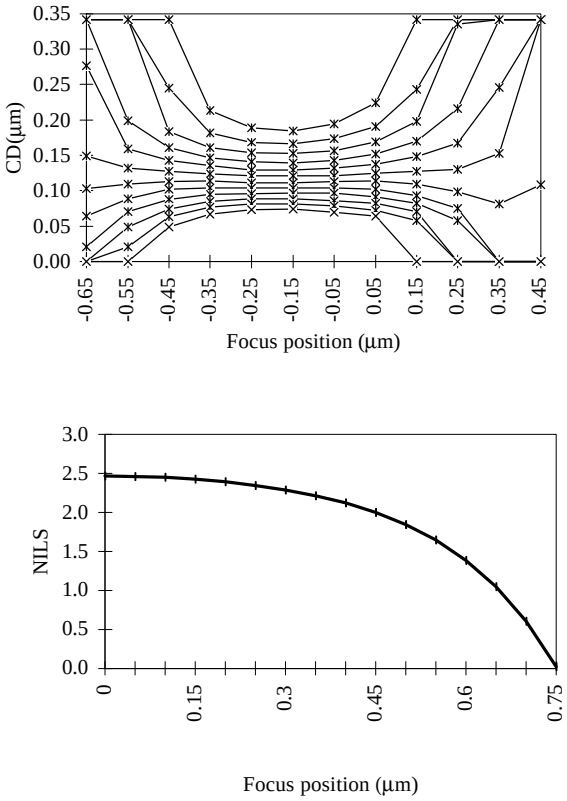

Figure 1. Determination of minimum NILS values for dense lines via focus exposure curves and aerial image / defocus relationships for 0.16 μm features (0.04 μm bias). Minimum NILS value is 2.4.

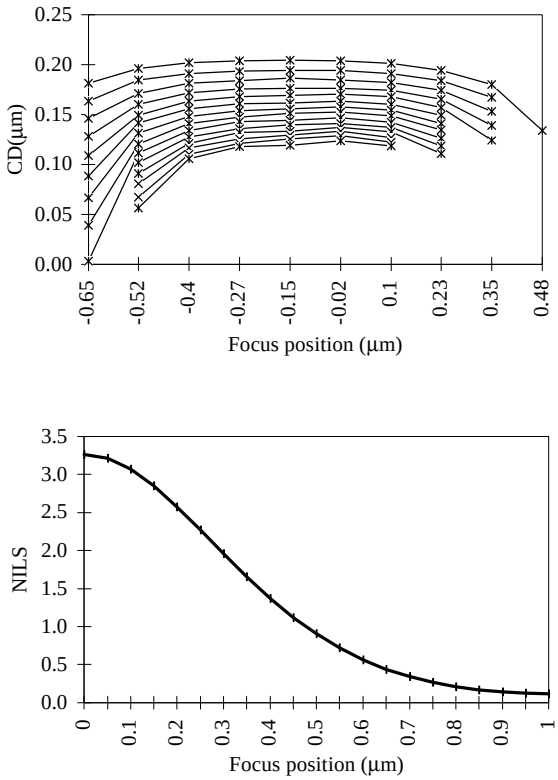

Figure 2. Determination of minimum NILS values for isolated lines via focus exposure curves and aerial image / defocus relationships for 0.16 μm features (0.02 μm bias). Minimum NILS value is 2.1.

3. 193nm SMALL FIELD CATADIOPTRIC LENSES EVALUATED

Evaluation of aberrations for three 193 nm, 0.6NA catadioptric lenses utilized in small field exposure systems is presented [7]. The lens schematic is shown in Figure 3. Performance has been evaluated through values of partial coherence and flare at nine field positions. Phase measurement interferometry (PMI) has allowed for wavefront description via 37 Zernike aberration coefficients for each field position. This lens design has made use of a beamsplitter incorporated into a lens element, known as a Mangin mirror. Here a partial reflector allows one element to act as both a reflector and a refractor. Although use of a Mangin mirror does require central obscuration (10% in this case), the impact on imaging are minimal if values are low [8]. Figure 4 shows how Strehl ratio is impacted by central obscuration for balanced primary aberrations: spherical, coma, astigmatism, defocus, and tilt. Strehl ratio can be estimated from the variance of particular aberrations using the approximation:

$$Strehl \sim \exp(-\sigma_{\phi}^{2})$$

At 10% obscuration, the impact on changes to Strehl ratio is low. Although the contribution of defocus, spherical, and balanced coma to Strehl degradation decreases with larger values, the detrimental effects from astigmatism and tilt above ~12% may be prohibitive.

Lithographic requirements of these lenses require that they allow resolution to 0.16 μm, demonstrate near diffraction limited depth of focus, provide performance for dense and isolated geometry, operate within specification across the full 2.1 mm field, exhibit flare below 2%, and print with H/V and isolated to dense bias values close to theoretical.

Figure 3. Schematic of small field 193nm catadioptric lens.

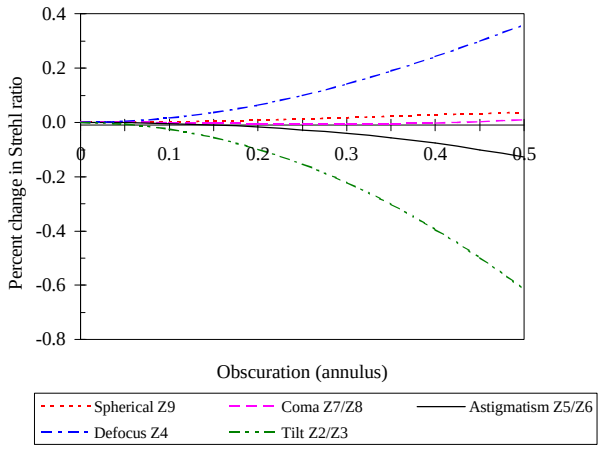

Figure 4. Influence of obscuration on balanced primary aberrations.

Evaluation has generated a significant amount of data for each lens set. Results presented here will be limited to two field positions and one orientation for 0.16 μm dense (1:1) and isolated features only. Further investigation has been performed using additional evaluation metrics (such as image placement error) and for contact and island features. Results will not be presented as specification for these attributes were not defined for these lenses.

Table 2 lists aberrations, Strehl ratio, and RMS OPD for the three lenses studied along with aberrations for a typical zone from lens design. It should be noted that lens set #2 is not a production lens and is included in this study for process validation.

Table 2. Aberration data for 193nm lens design and three lens sets. Strehl and RMS OPD are shown for each.

4. PERFORMANCE PREDICTIONS FOR 193nm LENSES

Figure 5 and 6 are contour plots of NILS value for 0.16 μm dense lines generated through scalar modeling of the lens from design. Figure 5 plots NILS vs. focus and partial coherence and Figure 6 plots NILS vs. focus and flare. The region corresponding to NILS values falling between 2.0 and 2.5 is highlighted. Aerial images that exhibit NILS values lower than this are not acceptable and fail to meet process requirements. A partial coherence near 0.7 appears optimum at 0.6 NA for these features and is used throughout for performance comparisons. As seen in Figure 6, flare levels above a few percent significantly degrade performance and focal depth (flare values for lenses studied measure below 2%). These contour plots allow determination of expected focal depth and can act as "fingerprints" for each field position of each lens. Figure 7 shows how lens set #1 compares with design in two field positions (best and worst of nine). Figure 8 shows results for lens set #2 and results for lens set #3 are shown in Figure 9.

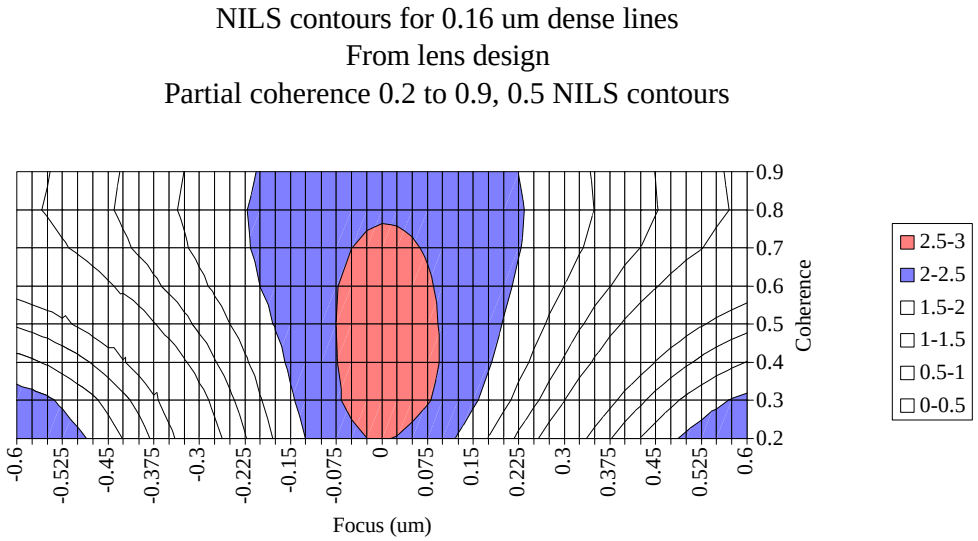

Figure 5.

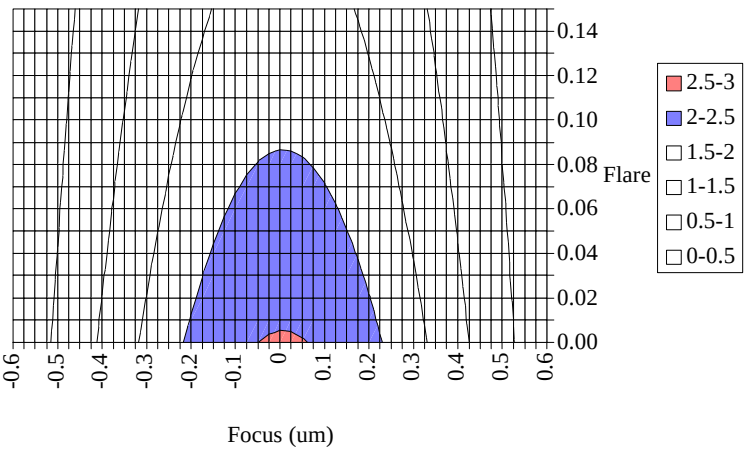

Figure 6.

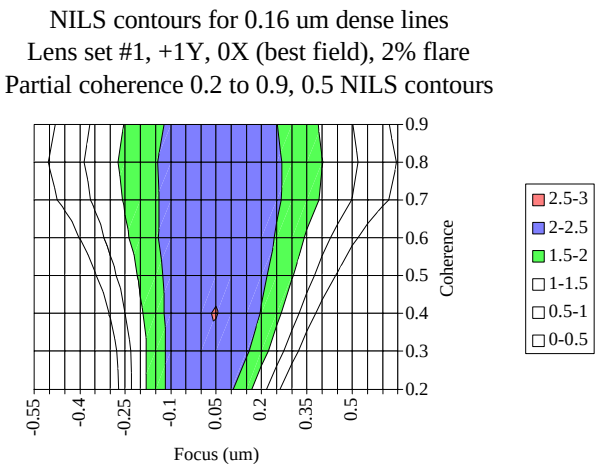

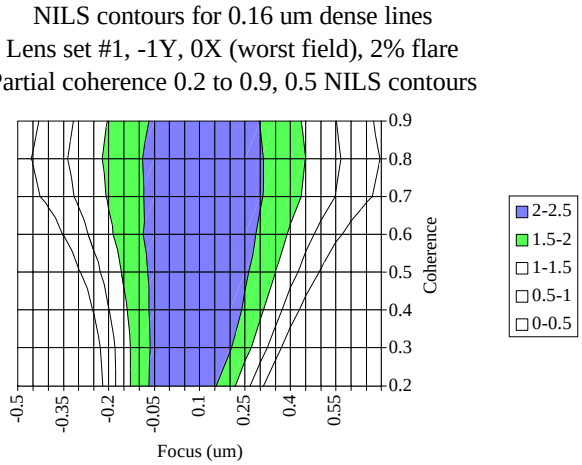

Figure 7.

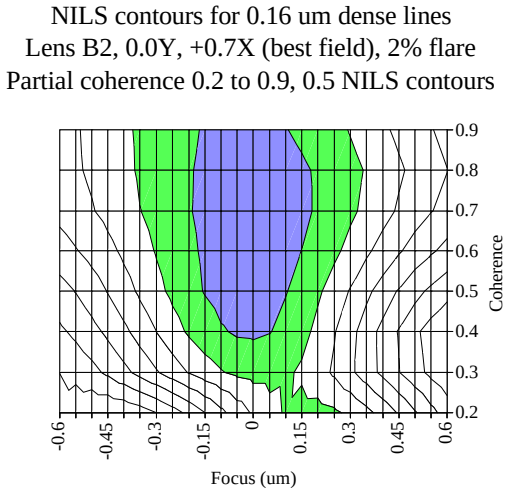

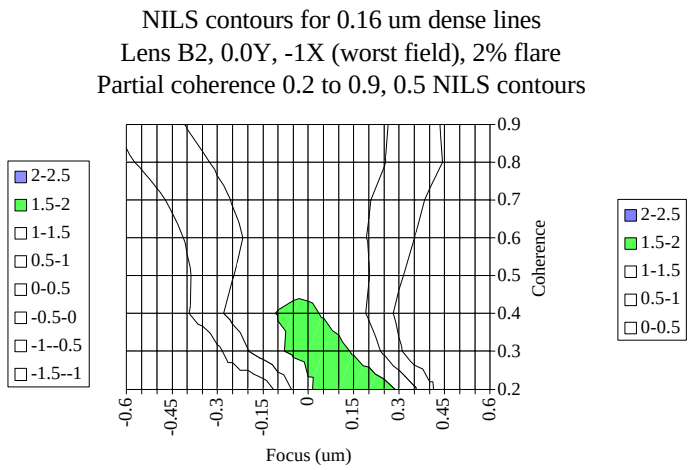

Figure 8.

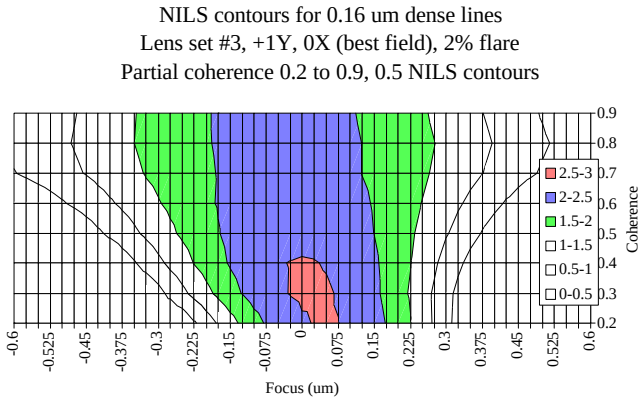

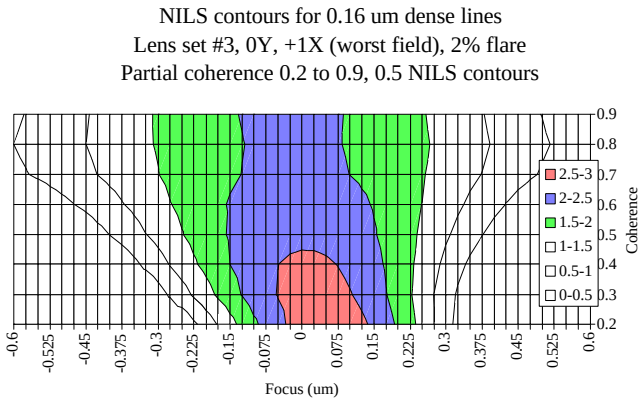

Figure 9.

The resulting projected usable focal depths for 0.16 μm dense features (at a partial coherence of 0.7) are listed in Table 3. The actual focal depth obtained through resist imaging is also included in this table for lens sets #2 and #3. Results are from an experimental single layer chemically amplified resist coated near 3000 Å over an organic ARC layer. Sizing criteria only was used for measured DOF. As seen from this data, predictions using the NILS metric closely match performance.

Resist NILS requirement	Lens #1 zones DOF (μm) best	worst	Test lens #2 zones DOF (μm) best	worst	Lens #3 zones DOF (μm) best	worst
2.0 minimum	0.38	0.32	0.34	0.00	0.35	0.25
1.5 minimum	0.64	0.62	0.64	0.00	0.63	0.55
Actual DOF			0.30	0.00	0.40	0.30

Table 3. Projected and actual depth of focus for 0.16 μm dense lines. The single layer resist process used for actual measurement has a corresponding minimum NILS requirements near 2.0.

Figure 10 and 11 are similar contour plots of NILS value for 0.16 μm isolated lines from the lens design. The region corresponding to NILS values falling between 2.0 and 2.5 is shown. These contour plots are now fingerprints of isolated line performance for various field positions of each lens. Figure 12 shows how lens set #1 compares with design in two field positions, Figure 13 shows results for lens set #2 and results for lens set #3 are shown in Figure 14. Table 4 summarizes predicted and actual DOF performance for these features.

Figure 10.

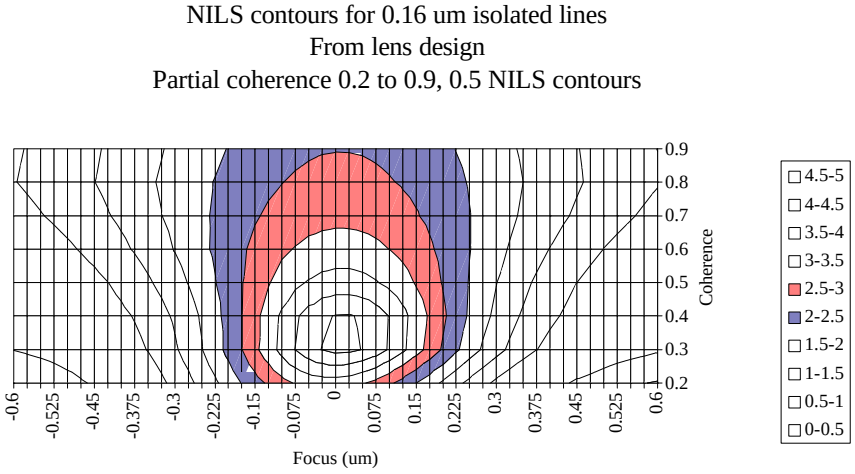

Figure 11.

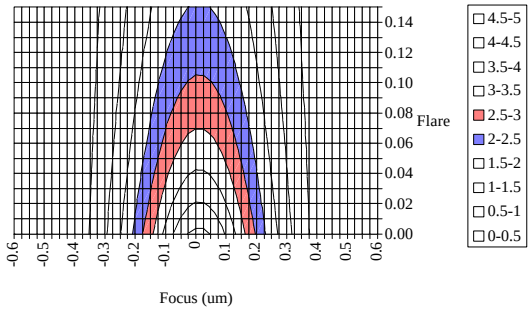

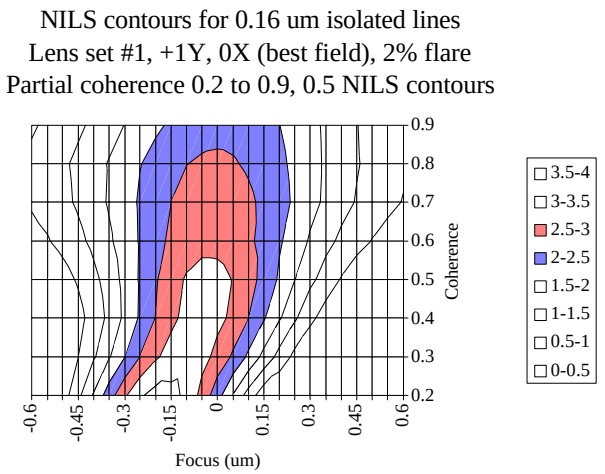

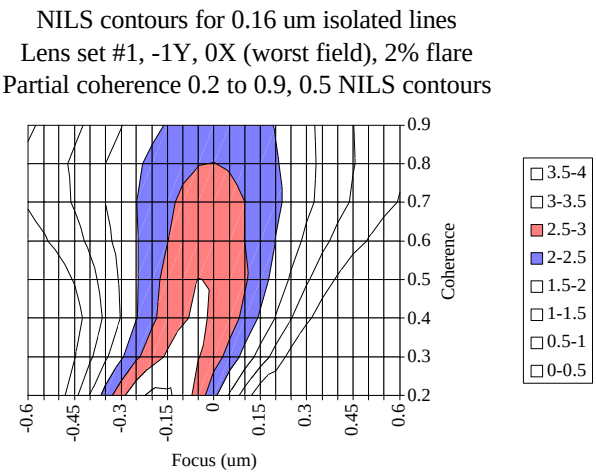

Figure 12.

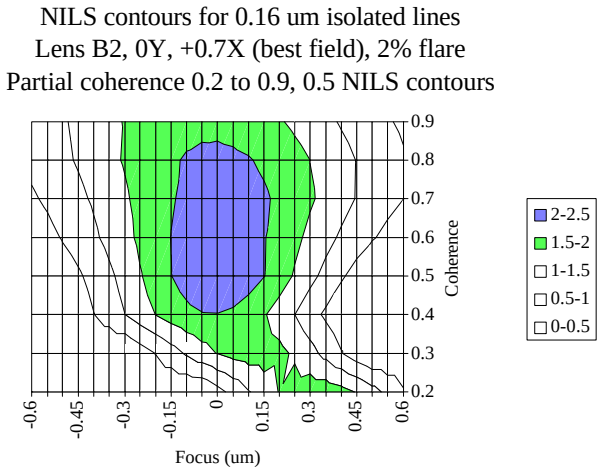

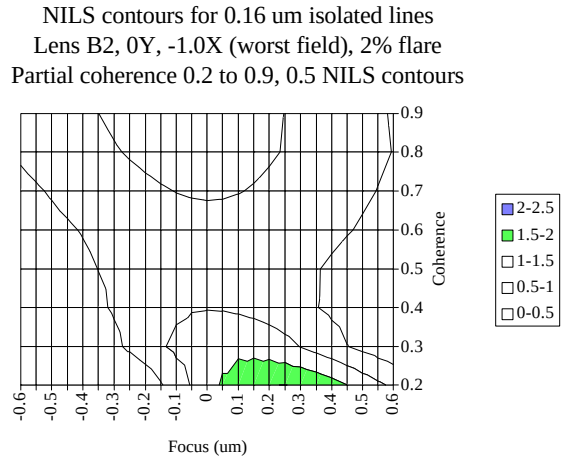

Figure 13.

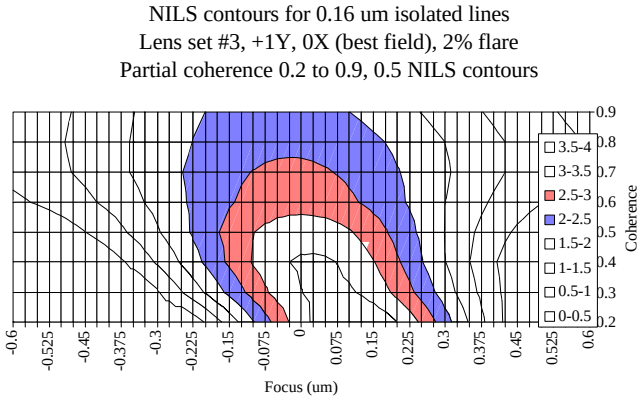

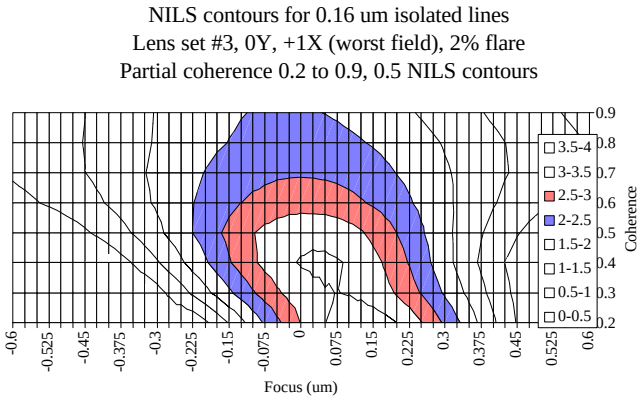

Figure 14.

Resist NILS requirement	Lens #1 zones DOF (µm) best	worst	Test lens #2 zones DOF (µm) best	worst	Lens #3 zones DOF (µm) best	worst
2.0 minimum	0.50	0.45	0.30	0.00	0.45	0.40
1.5 minimum	0.70	0.48	0.60	0.00	0.67	0.64
Actual DOF			0.30	0.00	0.50	0.40

Table 4. Projected and actual depth of focus for 0.16 µm isolated lines. The single layer resist process used for actual measurement has a corresponding minimum NILS requirements near 2.0.

Performance predictions were extended to smaller geometry using these same methods. Figure 15 and 16 show dense and isolated line performance for features from 0.18 to 0.12 µm in size for lens set #3. Current actual DOF performance of this lens for these feature sizes corresponds closely to the values predicted. Using a single layer resist and no resolution enhancement techniques, dense feature resolution to 0.14 µm can be achieved and isolated line performance to 0.13 µm is possible using the criteria outlined above. Geometry as small as 0.11 µm can also be printed but without significant DOF or image integrity.

NILS contours for 0.12 to 0.18 um dense lines
Lens set #3, +1.0Y, 0X (best) field,
0.70s, 2% flare, 0.50 NILS contours

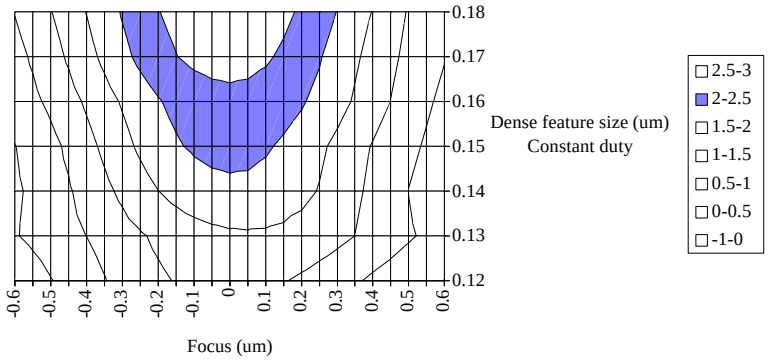

Figure 15.

NILS contours for 0.12 to 0.18 um isolated lines
Lens set #3 +1.0Y, 0X (best) field,
0.70s, 2% flare, 0.5 NILS contours

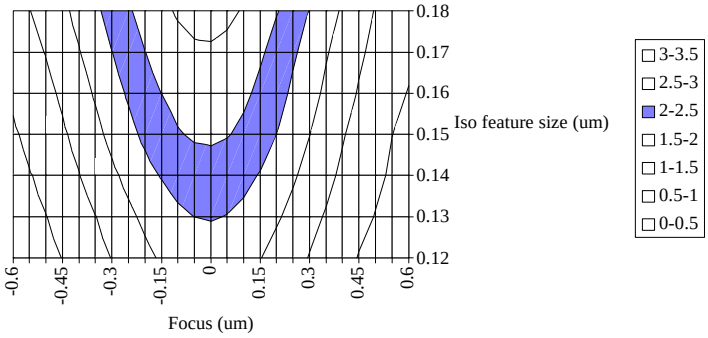

Figure 16.

5. IMPACT OF OFF-AXIS ILLUMINATION ON ABERRATION

It is anticipated that resolution enhancement techniques such as off-axis illumination will be needed to image geometry toward the 0.13 μm technology node projected for 193nm lithography. As these activities are explored, an understanding of their impact on aberrations is important. Figure 17 shows how quadrupole illumination can modify the aberrated behavior of a lithographic lens. Shown here are simulations of 0.16 μm dense lines imaged with a perfect lens and in the worst field position of the test lens #2 with conventional partial coherence (σ=0.7). Degradation through focus for the aberrated lens is as described previously. Shown also on this plot is NILS through focus for illumination with a quadrupole configuration with a center sigma of 0.8 and a radius sigma of 0.2. Comparison of the aberrated lens and the perfect lens indicate a reduction in image degradation through focus.

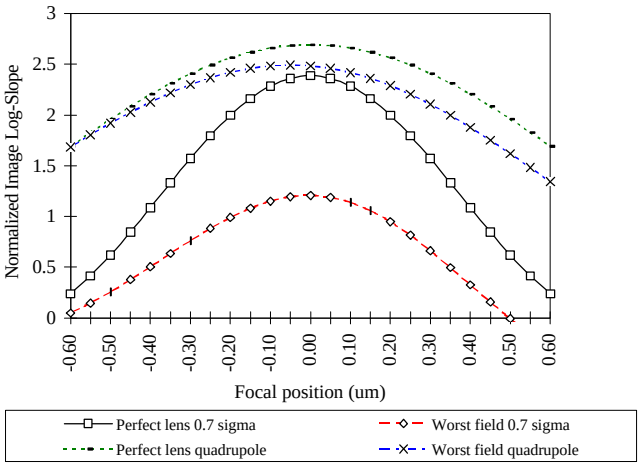

Figure 17. Quadrupole (0.8/0.2) and conventional (σ=0.7) of 0.16 μm dense (1:1) features. Aberration present in worst field case is predominantly coma.

These effects can be described using the diagram in Figure 18. Depicted here is the placement of overlapping zero and first diffraction orders within the objective lens pupil resulting from off-axis illumination. The full objective lens pupil is not fully utilized [9]. Instead, only a radial "ring" is utilized, determined by quadrupole sigma or annulus radii values Aberration terms (Zernike polynomials) can be modified as functions of ε1 and ε2 where:

$$\sigma_c=(\varepsilon_1+\varepsilon_2)/2$$
$$\sigma_r = (\varepsilon_1-\varepsilon_2)/2 \ .$$

Figure 18. The distribution of zero and first diffraction orders within the objective lens pupil for quadrupole illumination. Only a ring of the pupil is utilized for optimally illuminated features.

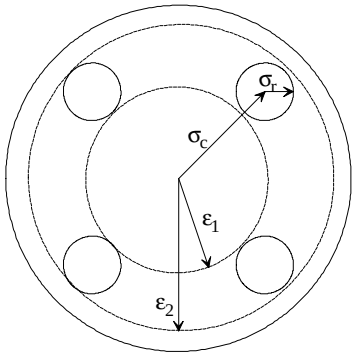

Modified Zernike polynomials orthogonal over this "ring" portion of the pupil can now be described in terms of ε1 and ε2. The standard deviation of aberrations allow for a description of the influence of OAI. Table 5 summarizes the standard deviation of balanced primary aberrations as functions of these defining parameters. Relationships are normalized to the peak aberration in each case. A more complete description is given in reference 9.

Aberration	Phase aberration $\Phi(r,\theta)$	Standard deviation of phase aberration / peak
Spherical	$Z_9\ [r^4 - (1 + \varepsilon_1)\ r^2]$	$\frac{\sqrt{5}}{30}\sqrt{16\varepsilon_2^4 - 2\varepsilon_1^2\varepsilon_2^2 - 30\varepsilon_2^2 + 15 + \varepsilon_2^4}\ (\varepsilon_2 - \varepsilon_1)(\varepsilon_2 + \varepsilon_1)$
Coma	$Z_{7,8}\ [r^3 - 2r/3(1+\varepsilon_1^{\ 2}+\varepsilon_1^{\ 4})(1+\varepsilon_1)]\cos\theta$	
Astigmatism	$Z_{5,6}\ [r^2(\cos^2\theta - 1/2)]$	$\frac{\sqrt{6}}{12}\sqrt{\varepsilon_2^4 + \varepsilon_1^2 + \varepsilon_1^4}$
Defocus	$Z_4\ [r^2]$	$\frac{\sqrt{3}}{6}\sqrt{\varepsilon_1^4 - 2\varepsilon_1^2\varepsilon_2^2 + \varepsilon_2^4}$
Tilt	$Z_{2,3}\ [r\cos\theta]$	$\frac{1}{2}\sqrt{\varepsilon_2^2 + \varepsilon_1^2}$

Table 5. Description of balanced primary aberrations and standard deviation/peak aberration within a ring determined by quadrupole parameters.

CONCLUSIONS

An approach has been introduced to establish tolerance limits for aberrations using a photoresist capability metric. This method has been shown to be sufficient to predict the performance of a lens system via an image log-slope metric and has allowed for the evaluation of 193 nm lithographic lenses without a fully developed resist process. Other aerial image metrics can be included to expand the capability of such an approach, such as image placement error, iso/dense bias, image intensity, or modulation. In general, it has been shown that lens aberration resulting in a Strehl ratio greater than 0.94 and RMS OPD of no more than 0.03 waves is adequate for imaging at pitch values at least as small as λ/NA [10].

ACKNOWLEDGMENTS

Shahid Butt, Intel Components Research (Joe Langston, Andrew Grenville, John Hutchinson), and ISI.

REFERENCES

1 Lord Rayleigh, Scientific Papers Vol. 1, Dover, New York, 1964, p. 432.
2 B.W. Smith, Microlithography: Science and Technology, Chapter 3: Optics for Photolithography, J.R. Sheats, B.W. Smith ed., New York: Marcel Dekker, 1998.
3 A. Hill, J. Webb., A. Phillips, J. Connors, SPIE Vol. 1927, (1993), 608.
4 L.A. Jones, J. Franklin Inst., 190, 39 (1920).
5 Prolith/2 version 5.
6 Prolith/2 parameter files courtesy of J. Byers, SEMATECH.
7 C. Sparkes, L. Thompson, R. Travers, Proc. SPIE Vol. 2726, 690 (1996).
8 J. Bruning, OSA Symposium on Design, Fabrication, and Testing for sub-0.25 micron Lithographic Imaging: Not published (1996).
9 B.W. Smith, L. Zavyalova, J. Petersen, Illumination pupil filtering using modified quadrupole apertures, Proc. SPIE Vol. 3334 (1998).
10 B.W. Smith, Revalidation of the Rayleigh resolution and DOF limits, Proc. SPIE Vol. 3334 (1998).